Transcriptional Response to Hypoxia in Human Tumors

Anita Lal, Hans Peters, Brad St. Croix, Zishan A. Haroon, Mark W. Dewhirst, Robert L. Strausberg, Johannes H. A. M. Kaanders, Albert J. van der Kogel, Gregory J. Riggins

Background: **The presence of hypoxic regions within solid tumors is associated with a more malignant tumor phenotype and worse prognosis. To obtain a blood supply and protect against cellular damage and death, oxygen-deprived cells in tumors alter gene expression, resulting in resistance to therapy. To investigate the mechanisms by which cancer cells adapt to hypoxia, we looked for novel hypoxia-induced genes.** ***Methods:*** **The transcriptional response to hypoxia in human glioblastoma cells was quantified with the use of serial analysis of gene expression. The time course of gene expression in response to hypoxia in a panel of various human tumor cell lines was measured by real-time polymerase chain reaction. Hypoxic regions of human carcinomas were chemically marked with pimonidazole. Immunohistochemistry and *in situ* hybridization were used to examine gene expression in the tumor's hypoxic regions.** ***Results:*** **From the 24 504 unique transcripts expressed, 10 new hypoxia-regulated genes were detected—all induced, to a greater extent than vascular endothelial growth factor, a hypoxia-induced mitogen that promotes blood vessel growth. These genes also responded to hypoxia in breast and colon cancer cells and were activated by hypoxia-inducible factor 1, a key regulator of hypoxic responses. In tumors, gene expression was limited to hypoxic regions. Induced genes included hexabrachion (an extracellular matrix glycoprotein), stanniocalcin 1 (a calcium homeostasis protein), and an angiopoietin-related gene.** ***Conclusions:*** **We have identified the genes that are transcriptionally activated within hypoxic malignant cells, a crucial first step in understanding the complex interactions driving hypoxia response. Within our catalogue of hypoxia-responsive genes are novel candidates for hypoxia-driven angiogenesis. [J Natl Cancer Inst 2001;93:1337–43]**

Normal tissues maintain a balance between cellular proliferation and oxygen supply. This balance is altered in solid human tumors, resulting in focal regions with oxygen levels far below those encountered in surrounding normal tissue *(1).* The cells in these regions either adapt to this hypoxic stress or die. Adaptation to a low-oxygen environment has serious consequences. For example, hypoxic tumor cells have a higher resistance to radiotherapy and certain chemotherapies *(2).* Hypoxia can promote a higher mutation rate *(3)* and select for a more metastatic and malignant phenotype *(4,5).* These observations raise the question: What are the molecular mechanisms by which cancer cells adapt to hypoxia and by which mechanisms do these detrimental effects occur?

An initial molecular response to hypoxia is increased levels of hypoxia-inducible factor 1 (HIF-1) protein *(6).* This transcription factor is a key regulator of hypoxia-driven apoptosis, growth arrest, and tumor vascularization. HIF-1 is also linked to oncogenesis by the von Hippel–Lindau tumor suppressor protein (vHL), which controls HIF-1 levels by proteolysis *(7).*

Reduced oxygen availability in the tumor can trigger a variety of cellular mechanisms, including cell cycle arrest, apoptosis, glycolysis, and angiogenesis. A powerful hypoxia-induced mitogen for endothelial cell growth is vascular endothelial growth factor (VEGF), which plays a critical role in the development of tumor vessels *(8).* In addition to hypoxia regulation, VEGF expression is stimulated by oncogenic mutations. Other important secreted proteins are angiopoietin family members. ANG2 causes reversion of vessels to a less differentiated state that promotes vessel remodeling *(8).* Inhibiting tumor angiogenesis provides an opportunity for therapy, and disruption of VEGF or its receptor is being evaluated *(9).* Genes yet to be discovered may influence angiogenesis in response to hypoxia, either in concert with these mitogens or separately.

To locate genes specific for hypoxic cells that contributed to angiogenesis or other pathologic effects of tumor hypoxia, we studied the global expression pattern of malignant cells by varying only oxygen concentration. A human glioblastoma multiforme (GBM) cell line was our hypoxia response model, since glioblastomas are rapidly proliferating brain tumors in which focal necrosis and extensive vascular proliferation are readily recognized *(10).* We used serial analysis of gene expression (SAGE) *(11)* for the initial comparison. SAGE allowed us to select the genes most potently induced by hypoxia from nearly all expressed genes. In addition to observing many known hypoxia-responsive genes, we identified a set of 10 novel hypoxia-inducible genes. Using real-time polymerase chain reaction (PCR) and *in situ* techniques on tumor sections, we also showed that these genes are often induced by hypoxia in a variety of solid tumors and specifically in the critical hypoxic regions of human tumors.

Materials and Methods

Cell Lines and Tumor Samples

Cell lines were grown with the use of standard cell culture techniques either in equilibrium with atmospheric oxygen or in an Environmental Chamber (Sheldon Manufacturing, Cornelius, OR) with 1.5% oxygen, which approximates the tumor hypoxia levels *(12)* for hypoxic conditions. Microelectrode measurements showed that diffusion of oxygen through the culture medium did not alter the oxygen concentration near the cells. In addition, no measurable change in the cell medium pH was detected after exposure to hypoxic conditions. Biopsy specimens of oropharyngeal carcinomas that were labeled with pimonidazole hydrochloride (Hypoxyprobe-1; Natural Pharmacia International Inc., Raleigh, NC) and iododeoxyuridine (IdUrd) were obtained during diagnostic examination of the patients under anesthesia after the patients gave written informed consent. Pimonidazole, a bioreductive marker, and IdUrd, an S-phase marker, were injected intravenously 2 hours and 20 minutes, respectively, before biopsy, as described previously *(13).* Institutional approval was obtained for this study. The panel of 17 cell lines represented short-term cultures of five

Affiliations of authors: A. Lal (Department of Pathology), Z. A. Haroon, M. W. Dewhirst (Department of Radiation Oncology), G. J. Riggins (Departments of Pathology and Genetics), Duke University Medical Center, Durham, NC; H. Peters, J. H. A. M. Kaanders, A. J. van der Kogel, Institute of Radiotherapy, University of Nijmegen, The Netherlands; B. St. Croix, The Johns Hopkins Oncology Center, The Johns Hopkins University School of Medicine, Baltimore, MD; R. L. Strausberg, Cancer Genomics Office, Office of the Director, National Cancer Institute, Bethesda, MD.

Correspondence to: Gregory J. Riggins, M.D., Ph.D., Cancer Genomics Laboratory, Duke University Medical Center, Box 3156, Durham, NC 27710 (e-mail: greg.riggins@duke.edu).

See "Notes" following "References."

GBMs, six medulloblastomas, two colon carcinomas, two breast carcinomas, and one non-small-cell lung cancer and short-term culture of one normal human astrocyte (Clonetics, Walkersville, MD).

Serial Analysis of Gene Expression

Messenger RNA (mRNA) was isolated from normal and hypoxic cells, and SAGE libraries were constructed as described previously *(11)*. Approximately 2000 plasmid clones from each library were purified and sequenced as part of the Cancer Genome Anatomy Project (CGAP) *(14)*. SAGE software v 3.04 (K. Kinzler, The Johns Hopkins Medical Institute, Baltimore, MD) was used to extract a total of 132 360 valid tags and to compare tag frequencies among libraries. Unique transcript tags were identified as described previously *(15)* with the use of an updated list of possible SAGE tags from the human transcriptome. Gene names and sequences were obtained by matching SAGE tags to the predicted SAGE tag from primate complementary DNA (cDNA) GenBank entries or human UniGene clusters that had a poly-A signal and/or a poly-A tail. Gene-expression increases predicted by SAGE were calculated by dividing the fraction of the particular SAGE tag in the hypoxic library by the fractional representation in the normal library. For tags not detected in normal oxygen, expression was set to one per 65 000 tags, the minimum detection level, to avoid division by zero. Complete SAGE tag counts are deposited at the CGAP SAGEmap web site (http://www.ncbi.nlm.nih.gov/SAGE/) under library names "SAGE Duke H247 normal" and "SAGE Duke H247 hypoxia."

Real-Time PCR and Western Blot Analysis

RNA from the various cell lines was purified and converted to cDNA with the use of random hexamer primers and reverse transcriptase to preserve the relative mRNA profile and produce a template suitable for PCR. Real-time PCR from this cDNA template was performed with the use of a thermocycler with continuous fluorescence-monitoring capabilities (LightCycler™; Roche Diagnostics, Indianapolis, IN) and SYBR® Green I (Molecular Probes, Eugene, OR) to analyze the kinetics of PCR product accumulation. PCR conditions and data analysis were reproduced as described previously *(16)* with the exception that 0.5 μ*M* PCR primer and 500 μ*M* of each deoxynucleoside triphosphate were used. Primers specific for a 221-base-pair (bp) segment of β-actin were used to confirm cDNA integrity and normalization of cDNA yields. Primers specific for each hypoxia-inducible gene were designed with 140- to 240-bp products (all primer sequences available upon request). The relative expression levels were determined in duplicate by comparison to a serially diluted standard with the use of the thermocycler software.

For western blot analysis, total cell lysates were prepared from cells grown either at normal oxygen or at 1.5% oxygen for the indicated times. Protein (75 μg) was separated by electrophoresis for each sample and was transferred to a polyvinylidenedifluoride membrane. The mouse monoclonal M75 antibody-containing lysate was diluted 1 : 5 and incubated with the membrane for 30 minutes, followed by incubation with horseradish peroxidase-conjugated goat anti-mouse immunoglobulin (Jackson ImmunoResearch Laboratories Inc., West Grove, PA). Bound antibody was visualized by chemiluminescence with the use of the SuperSignal West Pico substrate (Pierce Chemical Co., Rockford, IL). The molecular weights were determined with the use of a prestained protein ladder.

HIF-1 Transfection

The D247-MG cell line was transfected in six-well plates with the use of Transfast (Promega Corp., Madison, WI) and a full-length cDNA clone for HIF-1α in pEBB plasmid (Novus Biologicals, Littleton, CO). A β-galactosidase expression plasmid was used for the negative control. The cells designated as hypoxic were cultured at normal oxygen conditions for 5 hours after transfection and were transferred to 1% oxygen conditions for 19 hours. Normal oxygen transfections were harvested 24 hours after transfection.

Immunohistochemistry

Immunohistochemical staining for CA9 was performed on 5- to 8-μm fresh frozen tissue sections with the use of the mouse monoclonal G250 antibody (gift of E. Oosterwijk, University Medical Center, Nijmegen, The Netherlands) at a dilution of 3.2 μg/mL. The slides were fixed with acetone and blocked with horse serum; they were then sequentially incubated at room temperature with primary antibody, biotinylated secondary antibody, and avidin–biotin horseradish peroxidase complexes. Bound antibody was detected with the use of 3,3′-diaminobenzidine and hydrogen peroxide, counterstained with 1% hematoxylin, and permanently mounted.

For visualization of pimonidazole and IdUrd, 5-μm sections were placed in precooled acetone at 4 °C for 10 minutes, air-dried, and rehydrated with phosphate-buffered saline (PBS). Tissue DNA was denaturated in 2 N HCl for 10 minutes. To neutralize pH, we rinsed the sections in 0.1 *M* Borax and then in PBS. Sections were incubated for 45 minutes at 37 °C with 1 μg/mL anti-IdUrd (clone IU-4, raised in mouse; Caltag Laboratories Inc., Burlingame, CA) and rabbit anti-pimonidazole 1 : 200 in polyclonal liquid diluent (PLD). Next, sections were incubated for 90 minutes at room temperature in goat anti-rabbit ALEXAFLUOR488 (Molecular Probes) and goat anti-mouse Cy3, both 1 μg/mL in PLD. Between incubations, the sections were rinsed in PBS and finally mounted with Fluorostab (Euro-Diagnostica, Arnhem, The Netherlands).

In Situ Hybridization

Nonradioactive *in situ* hybridization was performed with the use of digoxigenin-labeled antisense RNA probes. PCR was used to generate 350- to 600-bp products specific to each hypoxia-overexpressed gene (HOG), and these products were subcloned into pBluescript KS– (Stratagene, La Jolla, CA). After growth in *Escherichia coli,* the plasmid was cut at a unique poly-linker site to create a linear probe. Digoxigenin-labeled RNA probes, from both the sense and the antisense strands, were generated with the use of the digoxigenin RNA-labeling reagents and either the T7 or the T3 polymerase (Roche Diagnostics). Alternatively, the T7 promoter was incorporated into an antisense primer, and the RNA probes were generated as described earlier *(17)*. Fresh, frozen sections were cut to 8 μm for *in situ* hybridization and processed as described previously *(17)*.

Statistical Analysis

SAGE software v 3.04 was used to calculate the statistical significance of the differences in the numbers of SAGE tags between hypoxic and normal libraries, based on a Monte-Carlo simulation as described previously *(18)* . The cutoff *P* values from this program were used as an aid to select candidate differentially expressed genes but were not relied on as evidence of differentially expressed genes, since this approach cannot account for errors in the mapping of tags to genes. A cutoff *P* value of .01 was used for consideration of a candidate hypoxia-induced gene. Although this level of significance introduced statistical false-positives when we considered 24 504 different transcripts (as compared with the usual, more restrictive level of $P<.001$), independent testing by real-time PCR (or published reports of hypoxia induction) was used to exclude these genes from Table 1 and from further analysis.

Results

Normal and Hypoxic Malignant Transcriptomes

To derive a model for the study of hypoxic expression changes, we cultured human glioblastoma cells either in 1.5% oxygen for 24 hours or in normal atmospheric oxygen. Real-time PCR analysis showed that three of 10 GBM cell lines induced VEGF transcript levels threefold or more (not shown), and one of them, D247-MG, was selected because it had the highest VEGF levels in response to hypoxia. Two SAGE libraries were constructed from hypoxic D247-MG cells and the normal oxygen control. A total of 132 360 SAGE tags were sequenced that clustered into 24 504 unique transcripts expressed. Between the two libraries, fewer than 0.5% of the genes had a statistically significant difference in expression.

We focused our analysis on the hypoxia-induced genes (Table 1), which included glycolytic enzymes, VEGF, and five other previously known hypoxia-responsive genes (referenced in Table 1). In addition, we identified 10 novel hypoxia-responsive genes. Some of these genes, such as the gene encoding the hepatic fibrinogen/angiopoietin-related protein (HFARP), have been investigated but have not been associated with hypoxia control. Three are novel genes that have only been identified as partially expressed sequence tags or cDNAs that encode for hypothetical proteins. We have designated these genes collectively as HOGs. There was no obvious amino acid sequence homology for the new HOGs to

Table 1. Genes induced by hypoxia in glioblastoma cell line D247-MG*

SAGE tag	Gene symbol (name)†	Accession No.‡	*P* value, SAGE	Fold increase, SAGE§	Fold increase, PCR§
GGACTTTCCT	NDRG1 (N-myc downstream-regulated 1, Cap43) *(37)*	D87953	.0023	12×	7.1×
TTTGTTAAAA	HOG18** (hypothetical protein FLJ20500)	NM_019058	.0074	10×	5.7×
GCCACGTTGT	HOG3** (hypothetical protein DKFZp434K1210)	NM_017606	.0021	9×	4.0×
GCTCCCCTGT	CA9 (carbonic anhydrase IX) *(23)*	NM_001216	.0021	9×	17×
GTGCTGGTGC	HFARP or PGAR** (hepatic fibrinogen/angiopoietin-related protein, PPAR-γ angiopoietin-related protein)	NM_016109	.0040	8×	12×
GTAATGACAG	STC1 (stanniocalcin 1)	NM_003155	.0040	8×	2.5×
CAGCCAAATA	HOG8** (3′ Ests only)	R51645	.0040	8×	2.1×
CTTAAGAAAA	MIG6** (mitogen-inducible gene-6)	AL137274	.0080	7×	2.5×
TGTTAGAAAA	PLOD2 (lysine hydroxylase 2)	NM_000935	.0027	5×	4.4×
GATAGCACAG	IGFBP5 (insulin-like growth factor-binding protein 5)	L27560	0	4×	4.6×
ATGTGTGTTG	BNIP3 (BCL2/adenovirus E1B 19-kd-interacting protein 3) *(35)*	NM_004052	.0009	4×	3.6×
ACTGAGGAAA	IGFBP3 (insulin-like growth factor-binding protein 3) *(38)*	NM_000598	0	3×	2.6×
AAGCTGTATA	HXB (hexabrachion, tenascin C)	NM_002160	.0071	3×	2.5×
GCTCTCTATG	SSR4 (translocon-associated protein delta)	NM_006280	.0018	3×	2.3×
TTTCCAATCT	VEGF (vascular endothelial growth factor) *(39)*	AF024710	.0048	3×	3.0×
GAAACAAGAT	PGK1 (phosphoglycerate kinase 1) *(40)*	NM_000291	0	2×	NT
GCGACCGTCA	ALDOA (aldolase A) *(40)*	NM_000034	0	2×	NT
TCTTGTGCAT	LDHA (lactate dehydrogenase A) *(40)*	NM_005566	0	2×	NT
AACGCGGCCA	MIF (macrophage migratory-inhibitory factor) *(38)*	NM_002415	.0001	2×	NT
TGAGGGAATA	TPI1 (triose phosphate isomerase 1) *(41)*	NM_000365	.0003	2×	NT

*SAGE = serial analysis of gene expression; PCR = polymerase chain reaction; NT = not tested; HOG = hypoxia-overexpressed gene; PPAR-γ = peroxisome proliferation-activated receptor-γ.

†Human Gene Nomenclature Database (www.gene.ucl.ac.uk/nomenclature/) symbols are provided or are marked (**) if not yet available. Genes already known to be induced by hypoxia are referenced.

‡GenBank or RefSeq accession number corresponds to the SAGE tag.

§Fold increases are the ratio of hypoxic to normal transcript levels for SAGE and real-time PCR.

other GenBank entries that might provide additional insight for gene function.

Confirmation, Time Course, and HIF-1 Response

From the 32 genes that were predicted by SAGE to be induced by hypoxia, 10 were reported previously as hypoxia induced, and there were 10 additional genes that we could confirm by real-time PCR. These 20 genes are shown in Table 1. Twelve genes predicted to be induced by SAGE were excluded from Table 1 because real-time PCR showed a less than twofold induction in a separate experiment (seven genes) or because we could not obtain a robust real-time PCR assay (five genes). Statistical false-positives in the SAGE data were not unexpected, since we used a high cutoff *P* value of .01 to locate more hypoxia-responsive genes.

A time course of induction was performed on 12 of the 20 verified hypoxia-inducible genes with the use of real-time PCR (Fig. 1, A). These genes all had a time course similar to that of VEGF, except for carbonic anhydrase IX (CA9), N-myc downstream-regulated 1 (NDRG1), HFARP, and hypothetical protein FLJ20500 (HOG18), which had a higher-fold induction of transcript levels. Most of the genes

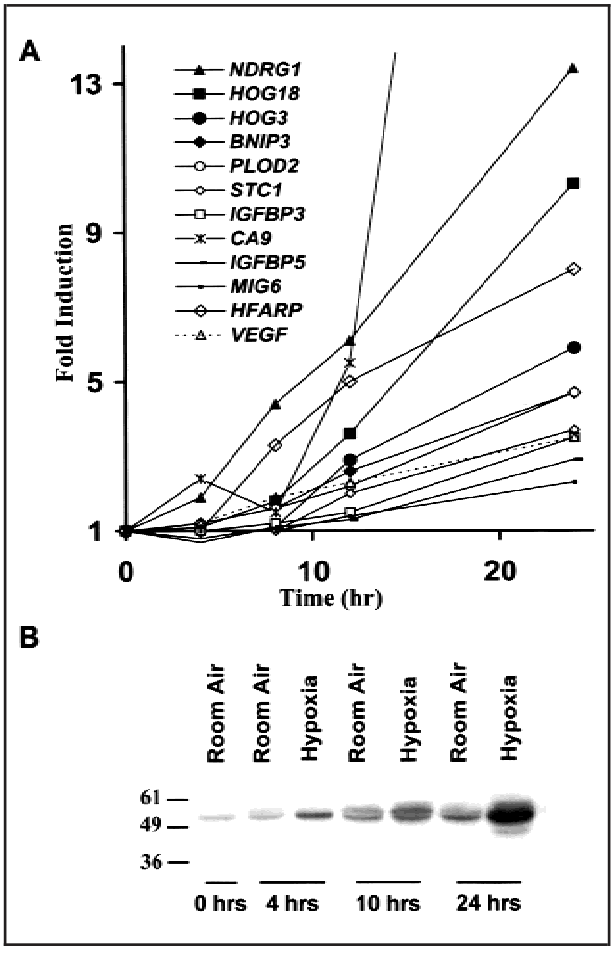

Fig. 1. Expression time course of hypoxia-overexpressed genes (HOGs) in 1.5% oxygen. **A**) Cultured glioblastoma cells (D247-MG) were switched to 1.5% oxygen at zero hours, and the levels of transcripts of the individual genes were determined by real-time polymerase chain reaction to produce the time course of hypoxia response. NDRG1 = N-myc downstream-regulated 1; HOG18 = hypothetical protein FLJ20500; HOG3 = hypothetical protein DKFZp434K1210;BNIP3 = BCL2/adenovirus E1B 19-kd-interacting protein 3; PLOD2 = lysine hydroxylase 2; STC1 = stanniocalcin 1; IGFBP3 = insulin-like growth factor-binding protein 3; CA9 = carbonic anhydrase IX; IGFBP5 = insulin-like growth factor-binding protein 5; MIG6 = mitogen-inducible gene-6; HFARP = hepatic fibrinogen/angiopoietin-related protein; VEGF = vascular endothelial growth factor. **B**) Protein expression time course of CA9 was measured by western blot analysis of D247-MG lysates from cells grown in atmospheric oxygen or in 1.5% oxygen. Molecular weight markers are shown **to the left.**

required a 12-hour exposure before appreciable hypoxia induction, implying an adaptation to chronic, rather than to acute, hypoxia. Western blot analysis, using an antibody to CA9, showed that protein levels were increasing, which was similar to the transcript level time course (Fig. 1, B).

We tested HOG18, hypothetical protein DKFZp434K1210 (HOG3), HFARP, CA9, insulin-like growth factor-binding protein 5 (IGFBP5), and insulin-like growth factor-binding protein 3 (IGFBP3) to see whether these genes might be regulated by HIF-1. VEGF, an HIF-1-regulated gene, was used as a positive control *(19)*. Standard transient transfection was able to insert the HIF-1α subunit gene plasmid (or a lac-Z control plasmid) into about 20% of the D247-MG cells, as demonstrated by β-galactosidase staining. All of the above genes showed a reproducible increase in expression due to HIF-1α at both atmospheric and 1% oxygen (Fig. 2, A).

HOG Induction in Other Common Cancers

The same 12 confirmed HOGs with time course data were assessed in a panel of 17 cell lines. We observed a hypoxia induction in many, but not in all, of the 12 genes, and the induction of these genes showed no tissue specificity (Fig. 2, B). Cultured normal human astrocytes were largely unresponsive, with only one gene induced over threefold compared with an average of 5.2 genes for the malignant cell lines.

CA9 had the greatest magnitude of induction among the 12 genes and was induced in the greatest number of tumor cell lines. A virtual northern blot analysis of 83 tumor and normal tissues archived at the CGAP SAGEmap database *(14)* showed that hypoxic D247-MG had the highest CA9 expression (>40 transcripts per cell). There was slight expression in three other tumors (<10 transcripts per cell), and there was no expression in 15 different types of untransformed adult cells. This pattern of expression is consistent with CA9 expression mainly in hypoxic malignant cells.

In Vivo Studies

Although the HOG response was reproducible in cancer cell lines, *in vivo* response in human solid tumors could differ. Pimonidazole *(20)* was used to accurately mark the hypoxic cells *(13)* of cervical or head and neck tumors. Staining of adjacent frozen sections allowed us to determine whether HOG expression colocalized with pimonidazole and other markers. Our first attempt showed a nearly identical expression pattern between pimonidazole and CA9 antibody staining in two squamous cell carcinomas from the oropharynx (Fig. 3, A, B, D, and F). In addition, expression of CA9 was not found in rapidly proliferating cells stained with IdUrd or in necrotic debris (Fig. 3, C). RNA *in situ* hybridization of NDRG1 also showed colocalization with hypoxia (Fig. 3, E and F). Similar results were obtained with cervical carcinomas (images not shown).

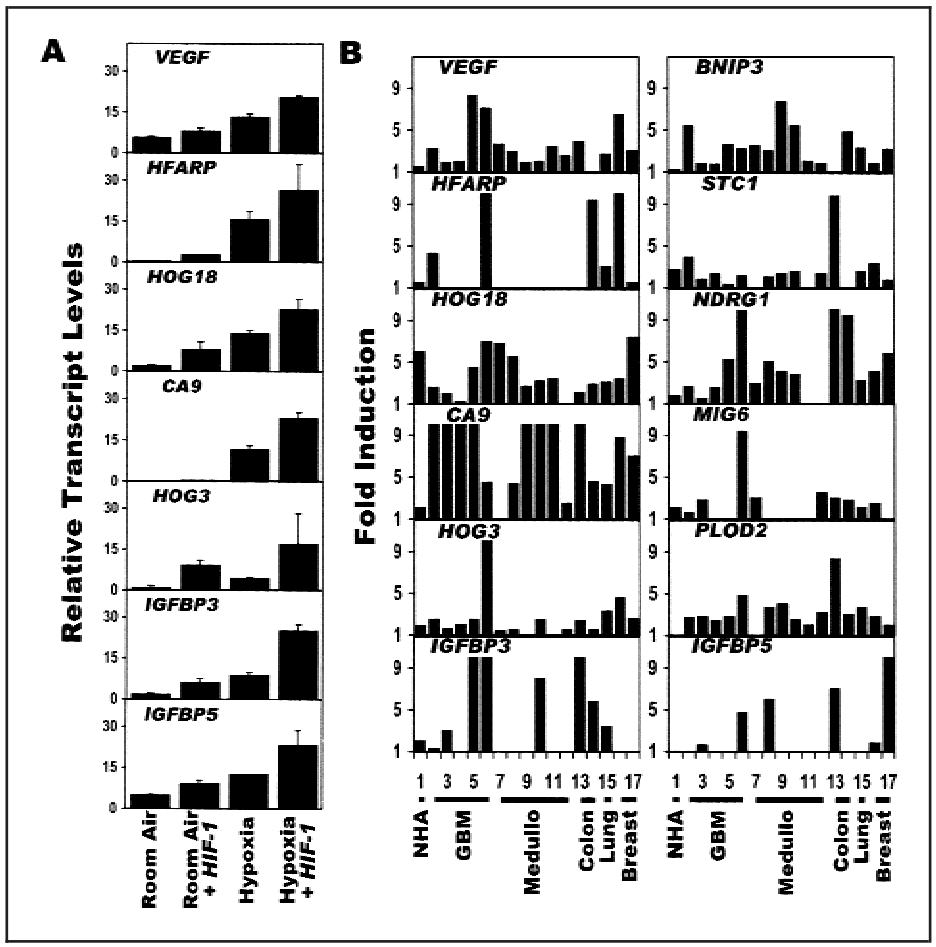

Fig. 2. Hypoxia-overexpressed gene (HOG) induction by hypoxia-inducible factor 1 (HIF-1) or hypoxia in malignant cells. **A**) D247-MG was transfected in triplicate with HIF-1α and cultured at either atmospheric or 1% oxygen to test HOG induction by HIF-1. Transcript levels are displayed as absolute values relative to the same standard as determined by real-time polymerase chain reaction (PCR), and **error bars** represent 95% confidence intervals. **B**) HOG induction in malignant cell lines derived from the commonly occurring cancers was determined by lowering the oxygen concentration from normal to 1.5% oxygen and measuring induction by real-time PCR. The 17 cell lines used were normal human astrocytes (NHA); glioblastomas multiforme (GBM) D263-MG, D392-MG, D502-MG, D566-MG, and U87; medulloblastomas D283-Med, D341-Med, D425-Med, D556-Med, D581-Med, and UW228; colon carcinomas SW480 and HCT116; non-small-cell lung carcinomas NCI-H23; and breast cancers SKBr3 and MCF7. Genes induced greater than 10-fold are displayed as 10-fold. VEGF = vascular endothelial growth factor; HFARP = hepatic fibrinogen/angiopoietin-related protein; HOG18 = hypothetical protein FLJ20500; CA9 = carbonic anhydrase IX; HOG3 = hypothetical protein DKFZp434K1210; IGFBP 3 = insulin-like growth factor-binding protein 3; IGFBP5 = insulin-like growth factor-binding protein 5; BNIP3 = BCL2/adenovirus E1B 19-kd-interacting protein 3; STC1 = stanniocalcin 1; NDRG1 = N-myc downstream-regulated 1; MIG6 = mitogen-inducible gene-6; PLOD2 = lysine hydroxylase 2.

The *in vivo* RNA expression pattern of HOGs was analyzed *in situ* in two glioblastomas, without the aid of the pimonidazole marker (Fig. 3, G–O). CA9 antibody stained live cells (Fig. 3, G and J) adjacent to necrotic regions in both tumors, showing that the CA9 staining was not an artifact of pimonidazole. Four more HOGs—BCL2/adenovirus E1B 19-kd-interacting protein 3 (BNIP3) (Fig. 3, H and K), NDRG1 (Fig. 3, I and L), HFARP (Fig. 3, O), and IGFBP3 (Fig. 3, M)—as well as VEGF showed this perinecrotic expression pattern. In addition to perinecrotic staining, IGFBP3 stained endothe-

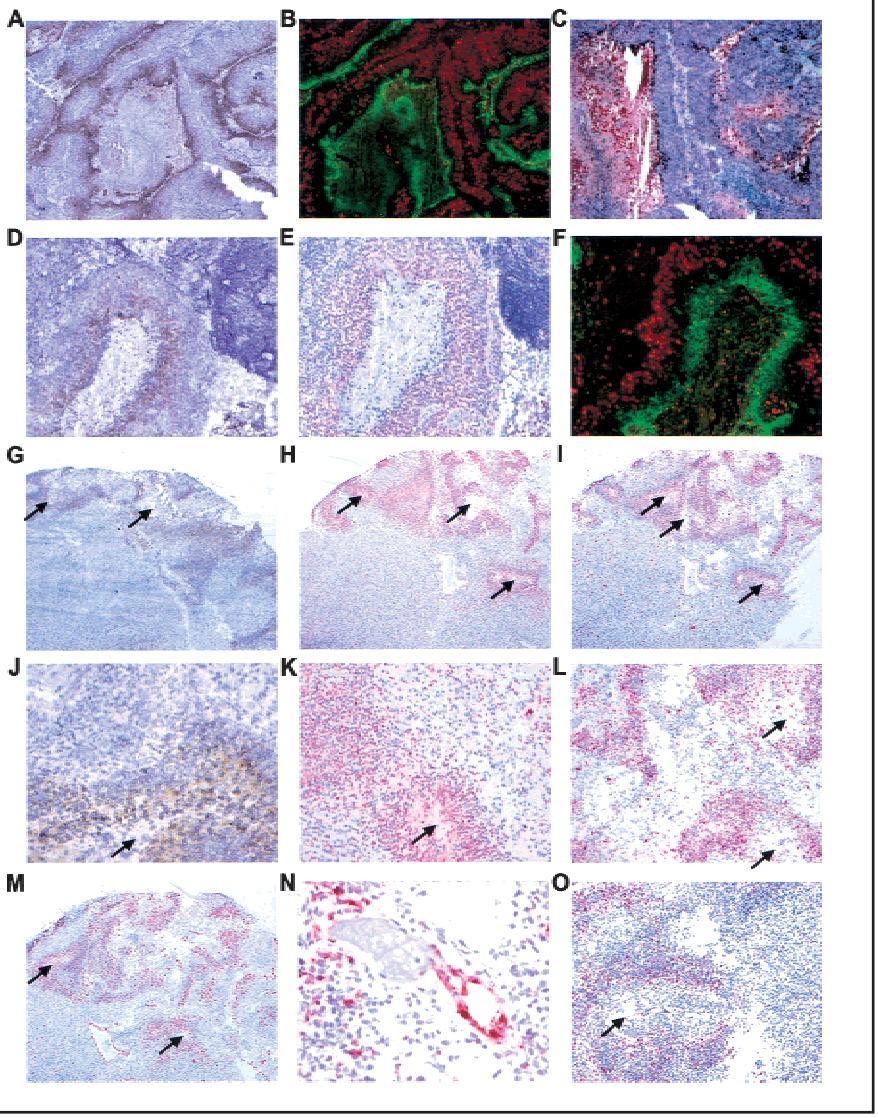

Fig. 3. *In vivo* expression of hypoxia-overexpressed genes in human solid tumors. Immunohistochemistry was used to colocalize carbonic anhydrase IX (CA9) (**A, brown stain**) and the chemical hypoxia marker pimonidazole (**B, green stain**) in serial sections of an oropharyngeal squamous cell carcinoma, sccNij70. **Regions staining red in panel B** represent proliferating (iododeoxyuridine-labeled) cells. A standard hematoxylin–eosin stain of an adjacent section (**C**) was used to show necrotic cells (**staining red**). *In situ* hybridization for N-myc downstream-regulated 1 (NDRG1) transcript (**E**) shows colocalization with CA9 (**D**) and pimonidazole (**F**) in an oropharyngeal squamous cell carcinoma. Perinecrotic staining in glioblastoma multiforme samples was observed for CA9 (**G** and **J**), for BCL2/adenovirus E1B 19-kd-interacting protein 3 (BNIP3) (**H** and **K**), for NDRG1 (**I** and **L**), for insulin-like growth factor-binding protein 3 (IGFBP3) (**M**), and for hepatic fibrinogen/angiopoietin-related protein (HFARP) (**O**). IGFBP3 stains endothelial cells in addition to hypoxic regions not adjacent to vessels (**N**). **Arrows** point to necrotic areas. Original magnifications ×10 for **panels A–C, G–I,** and **M;** ×25 for **panels D–F, L,** and **O;** ×50 for **panels J** and **K;** and ×100 for **panel N.**

lial cells (Fig. 3, N), but this was the only time high HOG expression was observed in nonhypoxic cells in tissue sections.

Discussion

A quantitative comparison was made between RNA expression levels in normal oxygenated and hypoxic human glioblastoma cells. Glioblastomas were chosen because they grow rapidly, show a high degree of neovascularization, and have readily identifiable regions of necrosis where VEGF is secreted. In a glioblastoma cell line that retained a VEGF response to hypoxia, we identified 20 HOGs, which include novel genes, genes encoding enzymes that hydrolyze sugar, angiogenic signaling genes, and apoptotic/stress-response genes. For 10 of the 20 HOGs, hypoxia response has not been reported previously, and induction was greater than that of VEGF. Brain, breast, colon, and lung cancer cell lines all responded to hypoxia; of six HOGs tested, all were HIF-1 controlled. *In situ* colocalization with pimonidazole showed distinct expression of CA9, NDRG1, and IGFBP3 in the hypoxic regions of human squamous cell and cervical carcinomas. Glioblastomas also showed expression of six tested HOGs in cells adjacent to necrotic foci.

CA9, a unique member of the carbonic anhydrase family, was the most consistently induced gene in this study, and expression of CA9 was not apparent in a wide survey of normal adult tissues. CA9 is a biomarker for renal cell and cervical carcinomas that is being targeted for therapeutic purposes *(21,22).* CA9 is regulated by vHL in renal cells through degradation of HIF-1α, is increased by vHL mutations, and shows perinecrotic staining in various tumors *(23,24).*

In addition to VEGF, several HOGs have a potential or documented role in angiogenesis. The angiopoietin-related gene (HFARP) encodes a secreted protein reported to protect endothelial cells from apoptosis *(25).* Although HFARP expression was originally thought to be limited to only a few tissues, this study shows that HFARP expression is hypoxia induced in commonly occurring cancers, which raises the possibility that interference with the secreted HFARP protein might inhibit angiogenesis in tumors.

Hexabrachion (HXB, tenascin C), an extracellular matrix glycoprotein, promotes endothelial cell sprouting with basic fibroblast growth factor *(26),* and expression is associated with angiogenesis in breast cancers, gliomas, and lymphomas *(27–29).* Antibodies specific to HXB can inhibit angiogenesis *(30),* and antisense therapy halts vascular thickening of pulmonary arteries *(31).*

Two insulin-like growth factor-binding proteins (IGFBP3 and IGFBP5), stanniocalcin 1 (STC1), and macrophage migratory-inhibitory factor (MIF) showed up as HOGs, with evidence pointing toward a function in endothelial cells, in addition to tumor cells. IGFBP3 was expressed in the endothelial cells of our tumors, and its expression in ovarian endothelial cells has been associated with vascular proliferation *(32).* IGFBP5 and STC1 were both identified as vascular endothelial cell markers in tumors *(17).* STC1 was induced during endothelial cell differentiation in an *in vitro* model *(33).* Anti-MIF

antibodies suppressed proliferation of endothelial cells and slowed the growth of murine adenocarcinomas *(34)*.

In addition to their role in angiogenesis, HOGs appear to be involved in modulating cell survival. BNIP3, a mitochondrial protein that activates apoptosis, was recently shown to be hypoxia controlled *(35)*. Another HOG, NDRG1, likely plays a role in cell cycle arrest and is mutated in a mendelian disorder, the Lom form of hereditary motor and sensory neuropathy (Online Mendelian Inheritance in Man OMIM Database #601455) *(36)*. Overall, the expression profile induced by hypoxia suggests a balance of signals regulating the cell cycle, apoptosis, and angiogenesis.

Cancers can adapt rapidly to environmental challenges, which partially explains why single-modality cancer therapy has not been as successful as multiagent therapy. This work documents a more complete set of genes whose function may be to allow the tumor to adapt to hypoxia. A practical application of these genes is as hypoxia-based prognostic markers. Some of the HOGs reported here should be more specific for hypoxic conditions in contrast to VEGF, which is expressed in normal tissues and undergoes substantial regulation independent of hypoxia. More importantly, the products from such genes may be tumor-specific targets for therapy. On the basis of the observation that many angiogenesis-related genes are hypoxia induced, it is possible that successful targeting of the right combination of HOGs could result in the disruption of the growth of blood vessels in tumors.

REFERENCES

(1) Thrall DE, Rosner GL, Azuma C, McEntee MC, Raleigh JA. Hypoxia marker labeling in tumor biopsies: quantification of labeling variation and criteria for biopsy sectioning. Radiother Oncol 1997;44:171–6.

(2) Brown JM. The hypoxic cell: a target for selective cancer therapy—eighteenth Bruce F. Cain Memorial Award lecture. Cancer Res 1999;59:5863–70.

(3) Yuan J, Narayanan L, Rockwell S, Glazer PM. Diminished DNA repair and elevated mutagenesis in mammalian cells exposed to hypoxia and low pH. Cancer Res 2000;60:4372–6.

(4) Hockel M, Schlenger K, Aral B, Mitze M, Schaffer U, Vaupel P. Association between tumor hypoxia and malignant progression in advanced cancer of the uterine cervix. Cancer Res 1996;56:4509–15.

(5) Rofstad EK. Microenvironment-induced cancer metastasis. Int J Radiat Biol 2000;76:589–605.

(6) Semenza GL. HIF-1: mediator of physiological and pathophysiological responses to hypoxia. J Appl Physiol 2000;88:1474–80.

(7) Maxwell PH, Wiesener MS, Chang GW, Clifford SC, Vaux EC, Cockman ME, et al. The tumour suppressor protein VHL targets hypoxia-inducible factors for oxygen-dependent proteolysis. Nature 1999;399:271–5.

(8) Yancopoulos GD, Davis S, Gale NW, Rudge JS, Wiegand SJ, Holash J. Vascular-specific growth factors and blood vessel formation. Nature 2000;407:242–8.

(9) Schlaeppi JM, Wood JM. Targeting vascular endothelial growth factor (VEGF) for antitumor therapy, by anti-VEGF neutralizing monoclonal antibodies or by VEGF receptor tyrosine-kinase inhibitors. Cancer Metastasis Rev 1999;18:473–81.

(10) Kleihues P, Burger PC, Collins VP, Newcomb EW, Ohgaki H, Cavenee WK. Glioblastoma. In: Kleihues P, Cavenee WK, editors. Pathology & genetics: tumours of the nervous system. Lyon (France): IARC Press; 2000. p. 29–39.

(11) Velculescu VE, Zhang L, Vogelstein B, Kinzler KW. Serial analysis of gene expression. Science 1995;270:484–7.

(12) Dewhirst MW, Ong ET, Klitzman B, Secomb TW, Vinuya RZ, Dodge R, et al. Perivascular oxygen tensions in a transplantable mammary tumor growing in a dorsal flap window chamber. Radiat Res 1992;130:171–82.

(13) Wijffels KI, Kaanders JH, Rijken PF, Bussink J, van den Hoogen FJ, Marres HA, et al. Vascular architecture and hypoxic profiles in human head and neck squamous cell carcinomas. Br J Cancer 2000;83:674–83.

(14) Lal A, Lash AE, Altschul SF, Velculescu V, Zhang L, McLendon RE, et al. A public database for gene expression in human cancers. Cancer Res 1999;59:5403–7.

(15) Velculescu VE, Madden SL, Zhang L, Lash AE, Yu J, Rago C, et al. Analysis of human transcriptomes. Nat Genet 1999;23:387–8.

(16) Loging WT, Lal A, Siu IM, Loney TL, Wikstrand CJ, Marra MA, et al. Identifying potential tumor markers and antigens by database mining and rapid expression screening. Genome Res 2000;10:1393–402.

(17) St Croix B, Rago C, Velculescu V, Traverso G, Romans KE, Montgomery E, et al. Genes expressed in human tumor endothelium. Science 2000;289:1197–202.

(18) Zhang L, Zhou W, Velculescu VE, Kern SE, Hruban RH, Hamilton SR, et al. Gene expression profiles in normal and cancer cells. Science 1997;276:1268–72.

(19) Ravi R, Mookerjee B, Bhujwalla ZM, Sutter CH, Artemov D, Zeng Q, et al. Regulation of tumor angiogenesis by p53-induced degradation of hypoxia-inducible factor 1alpha. Genes Dev 2000;14:34–44.

(20) Raleigh JA, Calkins-Adams DP, Rinker LH, Ballenger CA, Weissler MC, Fowler WC Jr, et al. Hypoxia and vascular endothelial growth factor expression in human squamous cell carcinomas using pimonidazole as a hypoxia marker. Cancer Res 1998;58:3765–8.

(21) Nogradi A. The role of carbonic anhydrases in tumors. Am J Pathol 1998;153:1–4.

(22) Uemura H, Nakagawa Y, Yoshida K, Saga S, Yoshikawa K, Hirao Y, et al. MN/CA IX/G250 as a potential target for immunotherapy of renal cell carcinomas. Br J Cancer 1999;81:741–6.

(23) Wykoff CC, Beasley NJ, Watson PH, Turner KJ, Pastorek J, Sibtain A, et al. Hypoxia-inducible expression of tumor-associated carbonic anhydrases. Cancer Res 2000;60:7075–83.

(24) Ivanov SV, Kuzmin I, Wei MH, Pack S, Geil L, Johnson BE, et al. Down-regulation of transmembrane carbonic anhydrases in renal cell carcinoma cell lines by wild-type von Hippel-Lindau transgenes. Proc Natl Acad Sci U S A 1998;95:12596–601.

(25) Kim I, Kim HG, Kim H, Kim HH, Park SK, Uhm CS, et al. Hepatic expression, synthesis and secretion of a novel fibrinogen/angiopoietin-related protein that prevents endothelial-cell apoptosis. Biochem J 2000;346 Pt 3:603–10.

(26) Schenk S, Chiquet-Ehrismann R, Battegay EJ. The fibrinogen globe of tenascin-C promotes basic fibroblast growth factor-induced endothelial cell elongation. Mol Biol Cell 1999;10:2933–43.

(27) Vacca A, Ribatti D, Fanelli M, Costantino F, Nico B, Di Stefano R, et al. Expression of tenascin is related to histologic malignancy and angiogenesis in b-cell non-Hodgkin's lymphomas. Leuk Lymphoma 1996;22:473–81.

(28) Jallo GI, Friedlander DR, Kelly PJ, Wisoff JH, Grumet M, Zagzag D. Tenascin-C expression in the cyst wall and fluid of human brain tumors correlates with angiogenesis. Neurosurgery 1997;41:1052–9.

(29) Tokes AM, Hortovanyi E, Kulka J, Jackel M, Kerenyi T, Kadar A. Tenascin expression and angiogenesis in breast cancers. Pathol Res Pract 1999;195:821–8.

(30) Canfield AE, Schor AM. Evidence that tenascin and thrombospondin-1 modulate sprouting of endothelial cells. J Cell Sci 1995;108(Pt 2):797–809.

(31) Cowan KN, Jones PL, Rabinovitch M. Elastase and matrix metalloproteinase inhibitors induce regression, and tenascin-C antisense prevents progression, of vascular disease. J Clin Invest 2000;105:21–34.

(32) Fraser HM, Lunn SF, Kim H, Duncan WC, Rodger FE, Illingworth PJ, et al. Changes in insulin-like growth factor-binding protein-3 messenger ribonucleic acid in endothelial cells of the human corpus luteum: a possible role in luteal development and rescue. J Clin Endocrinol Metab 2000;85:1672–7.

(33) Kahn J, Mehraban F, Ingle G, Xin X, Bryant JE, Vehar G, et al. Gene expression profiling in an *in vitro* model of angiogenesis. Am J Pathol 2000;156:1887–900.

(34) Ogawa H, Nishihira J, Sato Y, Kondo M, Takahashi N, Oshima T, et al. An antibody for macrophage migration inhibitory factor suppresses tumour growth and inhibits tumour-associated angiogenesis. Cytokine 2000;12:309–14.

(35) Bruick RK. Expression of the gene encoding the proapoptotic Nip3 protein is induced by

hypoxia. Proc Natl Acad Sci U S A 2000;97: 9082–7.

(36) Kalaydjieva L, Gresham D, Gooding R, Heather L, Baas F, de Jonge R, et al. N-myc downstream-regulated gene 1 is mutated in hereditary motor and sensory neuropathy-Lom. Am J Hum Genet 2000;67:47–58.

(37) Salnikow K, Blagosklonny MV, Ryan H, Johnson R, Costa M. Carcinogenic nickel induces genes involved with hypoxic stress. Cancer Res 2000;60:38–41.

(38) Koong AC, Denko NC, Hudson KM, Schindler C, Swiersz L, Koch C, et al. Candidate genes for the hypoxic tumor phenotype. Cancer Res 2000;60:883–7.

(39) Shweiki D, Itin A, Soffer D, Keshet E. Vascular endothelial growth factor induced by hypoxia may mediate hypoxia-initiated angiogenesis. Nature 1992;359:843–5.

(40) Semenza GL, Roth PH, Fang HM, Wang GL. Transcriptional regulation of genes encoding glycolytic enzymes by hypoxia-inducible factor 1. J Biol Chem 1994;269:23757–63.

(41) Niitsu Y, Hori O, Yamaguchi A, Bando Y, Ozawa K, Tamatani M, et al. Exposure of cultured primary rat astrocytes to hypoxia results in intracellular glucose depletion and induction of glycolytic enzymes. Brain Res Mol Brain Res 1999;74:26–34.

NOTES

Supported by Public Health Service National Cancer Institute (NCI)–Cancer Genome Anatomy Project (CGAP) contract No. S98–146 from the NCI, National Institutes of Health, Department of Health and Human Services, and by a James S. McDonnell Foundation Scholarship (to G. J. Riggins).

We thank Rick Klausner (NCI, Bethesda, MD) for CGAP planning and administration, Christa Prange (Lawrence Livermore National Laboratory, Livermore, CA) for robotic arraying of CGAP libraries, Jeff Touchman (National Institutes of Health Intramural Sequencing Center, Gaithersburg, MD) for library sequencing (NIH intramural sequencing core), Gerard Bouffard (National Institutes of Health Intramural Sequencing Center) for sequence data processing, Alex Lash (National Center for Biotechnology Information, Bethesda) for informatics and web applications, Roger McLendon (Duke University Medical Center, Durham, NC) for assistance with histopathology, Egbert Oosterwijk (University Medical Center, Nijmegen, The Netherlands) for CA9 antibodies, and Linda Cleveland and Jie Li (Duke University Medical Center) for technical assistance.

Manuscript received February 20, 2001; revised June 18, 2001; accepted June 25, 2001.